2. B. Dünweg (2000) *Computer Simulationen zu Phasenübergängen und Kritischen Phänomenen*, Habilitationsschrift, U. Mainz
3. X. Zhu, F. Tavazza, D. P. Landau, and B. Dünweg (2005) *Phys. Rev. B* **72**, p. 104102
4. P. N. Keating (1966) *Phys. Rev.* **145**, p. 627
5. M. Laradji, D. P. Landau, and B. Dünweg (1995) *Phys. Rev. B* **51**, p. 4898
6. F. H. Stillinger and T. A. Weber (1985) *Phys. Rev. B* **31**, p. 5262
7. K. Hukushima and K. Nemoto (1996) *Phys. Soc. of Japan* **65**, p. 1604
8. R. H. Swendsen and J. S. Wang (1986) *Phys. Rev. Lett.* **57**, p. 2607
9. E. M. Vandeworp and K. E. Newman (1995) *Phys. Rev. B* **52**, p. 4086; E. M. Vandeworp and K. E. Newman (1997) *Phys. Rev. B* **55**, p. 14222
10. A. M. Ferrenberg and R. H. Swendsen (1989) *Phys. Rev. Lett.* **63**, p. 1195
11. V. Privman (Ed.) (1990) *Finite Size Scaling and Numerical Simulation of Statistical Systems*. World Scientific, Singapore
12. J. Adler, A. Hashibon, and G. Wagner (2002) *Recent Developments in Computer Simulation Studies in Condensed Matter Physics, XIV*, ed. D. P. Landau, S. P. Lewis, and H.-B. Schüttler, Springer, Heidelberg, p. 160
13. J. Adler (2003) *Comput. in Sci. and Engineering* **5**, p. 61
14. F. Tavazza, D. P. Landau, and J. Adler (2004) *Phys. Rev. B* **70**, p. 184103
15. This prediction was based upon the assumption (2) that the interfacial tension between the Si-rich and Ge-rich phases is finite. This assumption has turned out to be wrong. This gives rise to a complete suppression of capillary waves [16], and also to a phase behavior which strongly differs from that assumed in 2
16. B. J. Schulz, B. Dünweg, K. Binder, and M. Müller (2005) *Phys. Rev. Lett.* **95**, p. 096101
17. L. Cannavacciuolo and D. P. Landau (2005) *Phys. Rev. B* **71**, p. 134104

Computer Simulation of Colloidal Suspensions

H. Löwen

Heinrich-Heine-Universität Düsseldorf, Universitätsstraße 1, 40225 Düsseldorf, Germany
hlowen @thphy.uni-duesseldorf.de

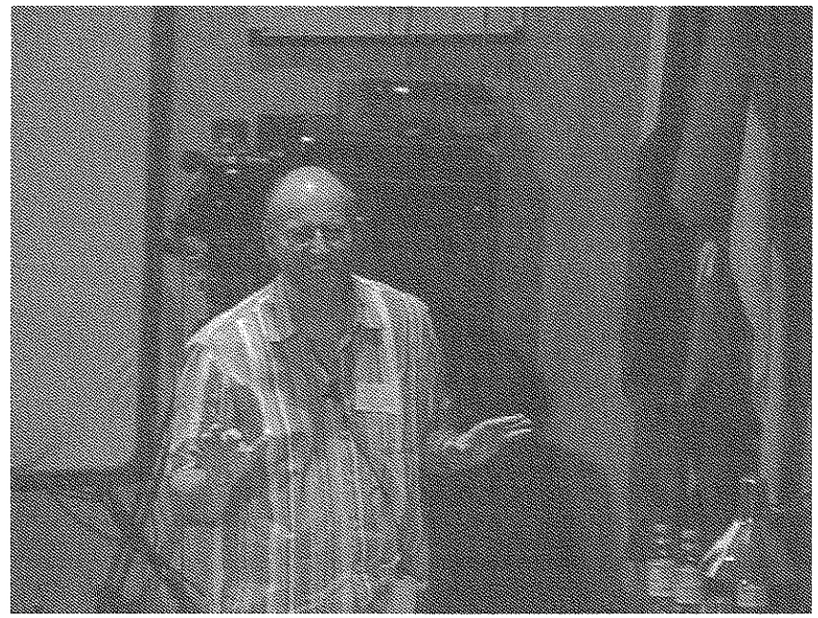

Hartmut Löwen

By definition, soft matter systems react sensitively upon external mechanical perturbations. This material class includes mesoscopic complex fluids such as colloidal suspensions. It is a major challenge to understand the fascinating properties of colloids from first principles, i.e., by deriving its properties from the microscopic interactions. Here, concepts borrowed from statistical physics are described, which are capable to overbridge the gap from microscopic over mesoscopic to macroscopic length scales. This is illustrated explicitly for charged colloidal suspensions and for star polymer solutions. A particular emphasis is placed on density functional theory.

1 Introduction

Soft matter [1] is synonymous with "complex fluids" and "colloids" although emphasis is put on different aspects in using these substitute names. The textbook definition of *colloids* is that there is at least one mesoscopic length scale in the range between 1nm and 1μm on which the system exhibit discontinuities. The main difference between a *molecular* and a *colloidal* system becomes immediately clear in comparing two liquids known from everyday life: water and milk. Water looks like a clear and structureless fluid on a length scale down towards nanometers and one needs molecular resolution to detect the water and alcohol molecules. Milk, on the other hand, consists of fat globules exhibiting already a structure on a length scale of 10 microns. Furthermore, milk contains submicron-sized caseine micelles which are the crucial building blocks in producing cheese. Hence the length scales of the characteristic structure are quite different in the two cases: water is a molecular and milk a colloidal liquid.

Discontinuities on a mesoscopic scale can happen between different phases. Accordingly [2], there are eight different kinds of colloidal dispersions depending on whether the disperse phase and the dispersion medium are in the solid, liquid or gas phase. The name "colloids" is also frequently used in a more specialized sense for colloidal suspensions which are solid particles embedded in a molecular liquid. Typical examples are printing ink, paints, blood, urine, spittle, adhesives (e.g. glue where the name "colloid" stems from), viruses, and muddy water.

The physics of colloids is the domain between molecular physics occuring on a length scale smaller than one nanometer and the traditional solid state physics of small crystallites which are larger than a micron. As a characteristic feature of colloids, their bulk to interface ratio is much larger than that of a crystallite. This can readily be seen by cutting a macroscopic solid into subunits and counting the resulting area. Hence colloidal and interfacial properties are very much inter-related.

If the term *complex fluids* is used, emphasis is put on the complexity of the description which involves very different (microscopic and mesoscopic) length scales. Finally, the expression *soft matter* puts emphasis on the mechanical

properties of colloidal materials. They react sensitively on mechanical perturbations as compression or shear. An example is given below.

Let us first focus on colloidal suspensions, i.e., solid mesoscopic particles embedded in a molecular solvent. A theorist would immediately approximate the solid colloidal particles by isotropic spheres. This is of course the leading order in a systematic approximation of the particle shape but it is not that crazy as it looks at a first glance. By sophisticated preparation methods one is nowadays indeed able to realize excellent model suspensions of monodisperse submicron-sized latex or polystyrol spheres [3]. For high colloidal concentrations, these spheres self-organize is crystalline arrays, i.e., they undergo a freezing transition. Such a colloidal crystal has a lattice constant a in the mesoscopic regime which leads to different elastic properties as compared to molecular solids. This is illustrated strikingly by considering the shear modulus G of a colloidal crystal. Roughly speaking, G scales with a typical energy scale (say the thermal energy k_BT) divided by a typical volume of the elementary crystal cell, $G \approx k_BT/a^3$. Hence a colloidal crystal has a shear modulus which is 9–12 orders of magnitude smaller than that of an ordinary crystal! This implies that colloidal crystals are vulnerable to shear and explains why the term "soft matter" is appropriate for colloidal samples.

Polymers are other prominent examples of soft matter. They are macromolecules composed of many monomeric units. A typical example is a linear hydrocarbon chain. But there are more complicated topologies conceivable, such as branched polymers (called dendrimers) or star polymers which consist of f linear chains attached to a common microscopic center [4]. The monomers can be charged resulting in a highly charged macromolecule which is called polyelectrolyte.

In this chapter I shall discuss systematic coarse-graining procedures which lead to effective interactions between the largest, mesoscopic particles in multicomponent, multiscale fluid mixtures. These effective interactions follow from a rigorous "integrating out" of microscopic degress of freedom. This concept allows for a simple understanding of trends in the phase behaviour, structure and dynamics of colloids and polymers. Moreover, the effective interaction can be used in standard simulations of samples involving only the large particles which now play the role of molecules in atomistic simulations. After a formal Statistical Mechanics justification of the coarse-graining procedure in Sect. 2, we shall briefly propose approximative density functional in Sect. 3 which are necessary to implement calculations within the coarse graining picture. The coarse graining concept will then be successively applied to interacting electric double-layers (Sect. 4), to solutions of star polymers (Sect. 5). A major part of this chapter (in particular that with an emphasis of computer simulations) is already published elsewhere in a recent review of the author Hansen [5]. Other useful review articles concerning the matter of effective interactions are those from Likos [6] and Belloni [7], aspects of charged suspensions are reviewed by Hansen and Löwen [8] and a recent review on computer simulations of colloids is provided by Dijkstra [9].

2 Effective Interactions

From a more theoretical point of view, the great challenge in soft matter is to understand and predict the macroscopic properties starting from the microscopic interactions. Already for pure molecular systems such an "ab initio" calculation poses a very hard problem. For a soft matter system this is even more complicated due to the presence of intermediate mesoscopic length scales.

Typical quantities of interest are the osmotic pressure of a colloidal dispersion, the elastic moduli or the phase behavior of colloidal suspensions as a function of internal thermodynamic or external parameters. A general framework to overbridge the different length scales is highly desirable because: i) a fundamental understanding of the thermodynamics of soft matter including biological macromolecules can be reached and ii) new material properties could be predicted.

It is clear that methods of classical equilibrium statistical mechanics should be applicable as most of the constituents are described as classical particles. Bridging the different length scales is most conveniently done in different steps from microscopic to mesoscopic and then from mesoscopic to macroscopic length scales. The first step can be made by using the important concept of the effective interaction. The second step is performed using ideas from classical many-body theory. Let us first outline these concepts briefly in general and then illustrate them for examples, in particular.

An efficient statistical description of multi-component systems involving particles of widely different sizes requires a controlled-coarse-graining which may be achieved by integrating ("tracing") out the degrees of freedom of the majority components of "small" particles, which may be solvent molecules, microscopic ions ("micro-ions") or monomers of macro-molecules. For the sake of simplicity, consider an asymmetric binary "mixture" of N_1 "large" spherical particles, with centres of positions $\{\boldsymbol{R}_i\}$ $(1 \le i \le N_1)$, and $N_2 \gg N_1$ "small" particles at positions $\{\boldsymbol{r}_j\}$ $(1 \le j \le N_2)$. Restriction will be made to thermodynamic equilibrium states. If classical statistics apply, integration over momenta is trivial, and the focus will be on configurational averages. The total potential energy of the mixture may be conveniently split ino three terms:

$$U(\{\boldsymbol{R}_i\},\{\boldsymbol{r}_j\}) = U_{11}(\{\boldsymbol{R}_i\}) + U_{22}(\{\boldsymbol{r}_j\}) + U_{12}(\{\boldsymbol{R}_i\},\{\boldsymbol{r}_j\}) \tag{1}$$

At a fixed inverse temperature $\beta = 1/k_BT$, the configurational part of the Helmholtz free energy F of the two-component system may be formally expressed as:

$$\begin{aligned} \exp(-\beta F) &= Tr_1\, Tr_2\, \exp(-\beta U) \\ &= Tr_1\, \exp(-\beta U_{11})\, Tr_2\, \exp(-\beta(U_{12}+U_{22})) \\ &= Tr_1\, \exp(-\beta U_{11})\, \exp(-\beta F_2(\{\boldsymbol{R}_i\})) \\ &= Tr_1\, \exp(-\beta V_{11}(\{\boldsymbol{R}_i\})) \end{aligned} \tag{2}$$

where the short-hand trace notation implies integration over the configuration space of species 1 or 2, i.e.

$$Tr_\alpha = \frac{1}{N_\alpha!}\int d^{3N_\alpha} r \tag{3}$$

$V_{11}(\{\boldsymbol{R}_i\})$, the effective interaction energy of the large particles, is the sum of their direct (or bare) interaction energy U_{11}, and of the configurational free energy of the fluid of small particles in the "external" field of the large particles F_2; the latter depends parametrically on the configuration $\{\boldsymbol{R}_i\}$ of the large particles

$$V_{11}(\{\boldsymbol{R}_i\}) = U_{11}(\{\boldsymbol{R}_i\}) + F_2(\{\boldsymbol{R}_i\}) \tag{4}$$

and can be written as:

$$F_2(\{\boldsymbol{R}_i\}) = -k_B T \ln[Tr_2 \exp(-\beta(U_{12}+U_{22})] \tag{5}$$

Up to now, no approximation has been made.

Three key aspects of the effective interaction V_{11} must be underlined. Firstly, *any* physical quantity $\mathcal{A}(\{\boldsymbol{R}_i\})$ depending only on the coordinates of the big particles can be formally averaged via the effective interaction

$$Tr_1 Tr_2 \mathcal{A}(\{\boldsymbol{R}_i\}) \exp(-\beta U) = Tr_1 \mathcal{A}(\{\boldsymbol{R}_i\}) \exp(-\beta V_{11}(\{\boldsymbol{R}_i\})) \tag{6}$$

Hence, once the effective interaction is known, any averages (e.g. pair correlations) of the big particles can be extracted directly.

Secondly, due to the presence of a free energy, F_2, V_{11} is obviously *state-dependent*, and has an entropic contribution of the small particles ($F_2 = U_2 - T S_2$).

Finally, although the direct interaction U_{11} may be pair-wise additive, this is no longer true of V_{11}. The free energy $F_2(\{\boldsymbol{R}_i\})$ generally has many-body-contributions, so that V_{11} will be of the more general form (with the change of notation $N_1 \to N$ and $V_{11} \to V_N$):

$$V_N(\{\boldsymbol{R}_i\}) = V_N^{(0)} + \sum_{i\le j}\sum v_2(\boldsymbol{R}_i,\boldsymbol{R}_j) + \sum_{i\le j\le k}\sum\sum v_3(\boldsymbol{R}_i,\boldsymbol{R}_j,\boldsymbol{R}_k) + \ldots . \tag{7}$$

$V_N^{(0)}$ is a state dependent but configuration-independent "volume" term, which has no bearing on the local structure of the large particles, but through its contribution to the thermodynamic properties, it can, in some cases, strongly influence their phase behaviour [10].

Let us now give some important examples of how to apply the concept of coarse-graining to soft matter systems. Obviously one has first of all to specify which statistical degrees of freedom should be considered and which of those should be integrated out ("small particles") and which of them should be left in the effective interaction ("big particles"). Depending on this choice

Table 1. Type of microscopic degrees of freedom which are integrated out for different kinds of macroparticles.

soft matter system	microscopic degrees which are coarse-grained	resulting physical effect
charged colloids	counterions, salt-ions	screening of Coulomb repulsions
polymers (linear chains, star polymers, dendrimers)	monomers	polymers viewed as soft spheres
colloid-polymer mixtures	polymer coils	depletion attraction between colloids
binary mixtures of big and small colloids	small colloids	depletion attraction and accumulation repulsion
nanoparticles in solvent	solvent particles	discrete solvent effects
polyelectrolyte stars	counterions, salt-ions	entropic interaction between centers

one can cover quite different physical phenomena which are summarized in Table 1. These include counterion screening of charged suspensions, depletion interactions in mixtures and polymer modeling by soft spheres. Most of those effects will be described in detail in the next sections.

Expression (4) for the effective interaction, or potential of mean force, was derived in the canonical ensemble, where the total numbers of small and large particles are fixed (closed system). In many practical situations the binary system is in osmotic equilibrium with a pure phase of the small particles (e.g the solvent), and the appropriate ensemble for such an open system is the semi-grand canonical ensemble where N_1 and the chemical potential μ_2 of the small particles (rather than N_2) are fixed. The corresponding thermodynamic potential is the semi-grand potential $\Omega_2 = \Omega_2(T, N_1, \mu_2; \boldsymbol{R}_i)$, and the effective interaction energy of the large particles will then be:

$$V_{11}(\boldsymbol{R}_i) = U_{11}(\boldsymbol{R}_i) + \Omega_2(\{\boldsymbol{R}_i\}) \tag{8}$$

which will again be state-dependent, a function of temperature, volume V and μ_2 (rather than $\rho_2 = N_2/V$).

In summary, the initial two-component system, involving a large number of microscopic degrees of freedom, has been reduced to an effective one-component system involving only the degrees of freedom of the mesoscopic particles. The price to pay is that the effective interaction energy is state-dependent and generally involves many-body terms. Approximations must now be invoked to calculate the highly non-trivial F_2 or Ω_2 term, i.e. the part of the interaction energy between the large particles induced by the small particles. Three different strategies have so far been used in practical implementations:

(a) For any given configuration $\{\boldsymbol{R}_i\}$ of the large particles, the small particles are subjected to the "external" potential $U_{12}(\{\boldsymbol{R}_i\},\{\boldsymbol{r}_j\})$, and hence form an inhomogeneous fluid, characterized by a local density $\rho(\boldsymbol{r};\{\boldsymbol{R}_i\})$. The thermodynamic potentials F_2 or Ω_2 are functionals of $\rho(\boldsymbol{r})$, and full use can be made of the classical density functional theory (DFT) of non-uniform fluids for the small particles [11,12]. DFT guarantees the existence of a excess free energy density functional $F_{exc}[\rho(\boldsymbol{r}]$ such that the free energies F_2 or Ω_2 can be written exactly as functionals:

$$F_2[\rho(\boldsymbol{r}] = F_{id}[\rho(\boldsymbol{r}] + F_{exc}[\rho(\boldsymbol{r}] + \sum_{j=1}^{N_1} \int \rho(\boldsymbol{r}) u_{12}(\boldsymbol{r}_i - \boldsymbol{R}_j)\, d\boldsymbol{r} \tag{9}$$

and

$$\Omega_2[\rho(\boldsymbol{r}] = F_2[\rho(\boldsymbol{r}] - \mu_2 \int \rho(\boldsymbol{r}) d\boldsymbol{r} \tag{10}$$

Here, $F_{id}[\rho(\boldsymbol{r}]$ is the functional of an ideal gas which is known exactly

$$F_{id}[\rho(\boldsymbol{r}] = k_B T \int \rho(\boldsymbol{r}) \left[\ln(\Lambda_2^3 \rho(\boldsymbol{r})) - 1\right] d\boldsymbol{r} \tag{11}$$

with Λ_2 being the thermal wave-length of the small particles. The density functionals given is (9) and (10) give the physical free energies F_2 or Ω_2 if the equilibrium density $\rho(\boldsymbol{r};\{\boldsymbol{R}_i\})$ of the small particles is inserted into the functional which follows from the variational minimization principle

$$\left.\frac{\delta\Omega_2[\rho^*(\boldsymbol{r})]}{\delta\rho^*(\boldsymbol{r})}\right|_{\rho^*=\rho} = 0 \tag{12}$$

where $\rho^*(\boldsymbol{r})$ is a properly parametrized trial density. The only difficulty is that in general the exact functional $F_{exc}[\rho(\boldsymbol{r}]$ is not known. Tractable approximations are known for hard spheres and soft potential fluids which are summarized in the next chapter. The optimization (12) may be implemented by steepest descent or conjugate gradient techniques, and the resulting effective potential energy between large particles can then be used directly in standard MC or MD simulations [13]. In the latter case, the forces $\boldsymbol{F}_i$ acting on the large particles may be directly calculated from a classical version of the Hellmann-Feynman theorem:

$$\begin{aligned}\boldsymbol{F}_i &= -\boldsymbol{\nabla}_i V_{11}(\{\boldsymbol{R}_j\}) \\ &= -\boldsymbol{\nabla}_i U_{11}(\{\boldsymbol{R}_j\}) - \langle \boldsymbol{\nabla}_i U_{12}(\{\boldsymbol{R}_j\},\{\boldsymbol{r}_l\})\rangle_{\{\boldsymbol{R}_j\}}\end{aligned} \tag{13}$$

where the angular bracket denotes an equilibrium average over the degrees of freedom of the small particles, for a forced configuration $\{\boldsymbol{R}_i\}$ of the large ones. If the interaction energy U_{12} between the two species is pairwise additive ($U_{12} = \sum_{i=1}^{N_1}\sum_{j=1}^{N_2} u_{12}(|\boldsymbol{r}_i - \boldsymbol{R}_j|)$), the force $\boldsymbol{F}_i$ is directly expressible in terms of the local equilibrium density $\rho(\boldsymbol{r})$:

$$\boldsymbol{F}_i = -\boldsymbol{\nabla}_i U_{11}(\{\boldsymbol{R}_j\}) - \int \rho(\boldsymbol{r})\, \boldsymbol{\nabla}_i u_{12}(\boldsymbol{r}_i - \boldsymbol{R}_j)\, d\boldsymbol{r} \tag{14}$$

The optimization can also be achieved "on the fly", along lines directly inspired by the Car-Parrinello method for ion-electron systems [14]. Successive minimization and large particle updating steps are replaced by a single dynamical evolution, which involves the physical motion of the large particles and fictitious dynamics of the local density of small particles, parametrized by a plane wave expansion [15].

(b) The previous DFT optimization method calculates directly the total effective energy of interaction between the large particles, or the resulting forces acting on each of these particles, without dividing V_N up into pair triplet and higher order interactions, as written in (7). Another strategy is to attempt to compute these various contributions separately. At very low concentration of large particles, the effective pairwise interaction v_2 is expected to be dominant. In order to map out v_2 as a function of the distance r between two large particles, one may use standard MC or MD algorithms to simulate a bath of small particles in the field of two fixed large particles. Equation (13) may then be used to calculate the mean forces acting on the two mesoparticles (which are opposite if the latter are identical) for each distance $r = |\boldsymbol{R}_1 - \boldsymbol{R}_2|$. The effective pair potential $v_2(r)$ finally follows from an integration of the forces. This procedure must be repeated for each distance r, but there are no time-scale or ergodicity problems, since the two large particles are fixed. The same goal can be achieved by appealing once more to DFT for the inhomogeneous fluid of small particles, subjected to the force field of two fixed large particles. The optimization may be carried out in r-space, using an adequate Eucledian or non-Eucledian [16] grid on which the local density of small particles is defined. For two identical large particles, the local density has obvious cylindrical symmetry, but under favourable conditions, a considerable simplification occurs by fixing one of the large particles and considering an infinitely dilute solution of large particles in a bath of small particles around the fixed large particle. The density profile of the large particles in the zero concentration limit is directly related to the effective pair potential between two large particles in a bath of small particles [17], i.e.,

$$v_2(r) = -k_B T \lim_{\rho_1 \to 0} \ln\left(\frac{\rho_1(r)}{\rho_1(r\to\infty)}\right) \tag{15}$$

The advantage is that the two density profiles $\rho_1(r)$ and $\rho_2(r)$ are now spherically symmetric, but the method requires the prior knowledge of an accurate density functional for an asymmetric binary mixture. This strategy may be generalized to the calculation of three-body and higher order effective interactions, by considering the density profiles of large and small particles around two or more fixed large particles [18].

(c) Although the effective interaction energy (4) or (8) is not, in general, pairwise additive at finite concentrations of the large particles, it would be

very convenient, for computational purposes, to reduce it, at least approximately, to a pairwise additive form. Contrarily to the two-body potential $v_2(r)$ discussed in the previous paragraph, which is only valid in the low density limit of large particles, the effective pair potential corresponding to finite concentrations is expected to be density-dependent, and will, in some average sense, incorporate the contributions of higher order terms in (7). Such effective density-dependent pair potentials can, in some cases, be derived from approximate functionals or from inversion procedures, examples of which will be described in Sect. 5.

3 Approximative Density Functionals

In this section we summarize different modern approximations for the excess free energy density functional $F_{exc}[\rho(\boldsymbol{r}]$ for different small-small interaction pair potentials $u_{22}(r)$, namely hard spheres and soft particles. The case of Coulomb interactions will be re-discussed in the next chapter.

For *hard spheres* of diameter σ the best current functional approximation is that of Rosenfeld's fundamental measure theory [19]. It can be constructed also for hard sphere mixtures but here we restrict ourselves to a one-component hard sphere fluid. In this approximation one takes

$$\mathcal{F}_{exc}[\rho] = k_B T \int d\boldsymbol{r} \Phi[\{n_\alpha(\boldsymbol{r})\}] \tag{16}$$

where one introduced a set of weighted densities

$$n_\alpha(\boldsymbol{r}) = \int_\Omega d\boldsymbol{r}' \rho(\boldsymbol{r}') w_\alpha(\boldsymbol{r} - \boldsymbol{r}') \tag{17}$$

Here, the index $\alpha = 0, 1, 2, 3, V1, V2$ labels six different weighted densities and six different associated weight functions. Explicitly these six weight functions are given by

$$w_0(\boldsymbol{r}) = \frac{w_2(\boldsymbol{r})}{\pi\sigma^2} \tag{18}$$

$$w_1(\boldsymbol{r}) = \frac{w_2(\boldsymbol{r})}{2\pi\sigma} \tag{19}$$

$$w_2(\boldsymbol{r}) = \delta\left(\frac{\sigma}{2} - r\right) \tag{20}$$

$$w_3(\boldsymbol{r}) = \Theta\left(\frac{\sigma}{2} - r\right) \tag{21}$$

$$w_{V1}(\boldsymbol{r}) = \frac{w_{V2}(\boldsymbol{r})}{2\pi\sigma} \tag{22}$$

and

$$w_{V2}(\boldsymbol{r}) = \frac{\boldsymbol{r}}{r}\delta\left(\frac{\sigma}{2} - r\right) \tag{23}$$

Note that the index V denotes a vector weight function. We can express this fact by writing $w_{V1} \equiv \boldsymbol{w}_{V1}$, $n_{V1} \equiv \boldsymbol{n}_{V1}$,... Finally the function Φ is given by

$$\Phi = \Phi_1 + \Phi_2 + \Phi_3 \tag{24}$$

with

$$\Phi_1 = -n_0 \ln(1 - n_3) \tag{25}$$

$$\Phi_2 = \frac{n_1 n_2 - \boldsymbol{n}_{V1} \cdot \boldsymbol{n}_{V2}}{1 - n_3} \tag{26}$$

and

$$\Phi_3 = \frac{n_3^2 (1 - (\boldsymbol{n}_{V2}/n_2)^2)^3}{24\pi(1 - n_3)^2} \tag{27}$$

The six weight functions are connected to the geometrical (fundamental) Minkowski measures [20]. There are several arguments in favor of the Rosenfeld approximation: as an example we mention that the freezing transition can be calculated by plugging in a constant density field for the fluid phase and a lattice sum of Gaussian peaks in the solid phase. If the width of the Gaussians and the prefactor are taken as variational parameters one gets a first-order freezing transition with coexisting packing fractions of $\eta_f = 0.491$ and $\eta_s = 0.540$ which are very close to "exact" simulation data $\eta_f = 0.494$, $\eta_s = 0.545$.

In the complementary case of very soft interactions, on the other hand, it has recently been shown that a mean-field approximation for the density functional is a very good approximation [21–23]. If the pair potential $u_{22}(r)$ is finite at the origin, then it can be shown that a mean-field functional is exact in the limit of very large densities. It works, however, amazingly well also for finite densities. In the mean-field approximation one takes:

$$\mathcal{F}_{exc}[\rho] = \frac{1}{2}\int d\boldsymbol{r} \int d\boldsymbol{r}' \rho(\boldsymbol{r})\rho(\boldsymbol{r}')u_{22}(|\boldsymbol{r} - \boldsymbol{r}') \tag{28}$$

All other intermediate cases are more difficult. Some success is to map harsh interaction onto effective hard spheres employing some ideas from the construction of Rosenfeld's functional [24]. Treating attractive tails has mainly been limiting to mean-field-like approaches as well.

4 Charged Colloidal Dispersions

Electric double-layers around mesoscopic colloidal particles of various shapes (spheres, rods, platelets, ...) or around polyelectrolytes make the generally dominant contribution to the effective interaction between highly-charged particles, which will be referred to as polyions [7,8]. Most simulations are based on a primitive model, whereby the discrete nature of the aqueous solvent is neglected, and a macroscopic value of the dielectric permittivity ϵ is assumed.

At very low polyion concentration, strategy b) of the previous section may be adopted to compute an effective pair interaction between two polyions, which is screened by microscopic counterions of opposite sign, as well as coions in the presence of added salt. The resulting effective pair potential turns out to be invariably repulsive of the screened Coulomb form predicted a long time ago by Derjaguin, Landau Verwey and Overbeek (DLVO) [25] as long as the microions are monovalent. However if divalent counterions are present, they are more strongly correlated, and this may lead to a short-range attraction between equally-charged polyions, due to an overscreening effect [26]. Although most of the work on effective pair interactions has focussed so far on spherical polyions, some recent MC simulations have investigated the case of lamellar colloids [27]. The triplet interaction between spherical polyions has similarly been calculated by MD simulations of co and counterions in the field of three fixed polyions [28], and turns out to be attractive under most circumstances. In the opposite limit of high concentrations, each polyion is confined to a cage of neighbouring polyions, so that many-body interactions are expected to be important, and pairwise additivity of the effective interaction is expected to break down. It is then reasonable to consider a Wigner-Seiz cell model, where a cell of geometry adapted to the shape of the polyions (e.g. a spherical cell for spherical polyions) contains one polyion at its centre, surrounded by co and counterions, such that overall charge neutrality is ensured, and with appropriate boundary conditions for the electric field on the surface of the cell. A physically reasonable boundary condition is to impose that the normal-component of the electric field vanishes on the surface. The initial problem involving many polyions is thus approximately reduced to the much simpler problem of a single polyion surrounded by its electric double-layer. Although all information on correlations between polyions is lost, the cell model allows a calculation of the thermodynamic properties of concentrated suspension, from MC or MD simulations of the inhomogeneous fluid of microions contained in the cell, as well as an estimate of the effective polyions charge, taking into account the phenomenon of counterion "condensation" [29, 30]. Such simulations provide stringent tests for approximate DFT calculations, including Poisson-Boltzmann (PB) theory.

At moderate polyion concentrations, the two previous strategies break down. Strategy a) of the previous section, based on the step by step or "on the fly" optimization of an appropriate free energy functional of the microion density profiles, is the most appropriate [15]. The free energy functional $F_2[\rho_+(\boldsymbol{r}), \rho_-(\boldsymbol{r}), \{\boldsymbol{R}_i\}]$ of the co- and counterion densities is conveniently split into ideal, Coulomb, external and correlation parts:

$$F_2[\rho_+, \rho_-] = F_{id}[\rho_+] + F_{id}[\rho_-] + F_{Coul}[\rho_c] + F_{ext}[\rho_+] + F_{ext}[\rho_-] + F_{corr}[\rho_+, \rho_-] \tag{29}$$

where:

$$F_{id}[\rho_\alpha] = k_B T \int \rho_\alpha(\boldsymbol{r}) \left[\ln(\Lambda_\alpha^3 \rho_\alpha(\boldsymbol{r})) - 1\right] d\boldsymbol{r} \tag{30}$$

$$F_{Coul}[\rho_\alpha] = \frac{e^2}{2} \int d\boldsymbol{r} \int d\boldsymbol{r}' \frac{\rho_c(\boldsymbol{r})\, \rho_c(\boldsymbol{r}')}{|\boldsymbol{r} - \boldsymbol{r}'|} \tag{31}$$

$$F_{ext}[\rho_\alpha] = \int \varphi_{ext}(\boldsymbol{r})\, \rho_\alpha(\boldsymbol{r})\, d\boldsymbol{r} = \sum_{i=1}^{N_1} \int u_{1\alpha}(\boldsymbol{r} - \boldsymbol{R}_i)\, \rho_\alpha(\boldsymbol{r})\, d\boldsymbol{r} \tag{32}$$

In (31), $\rho_c(\boldsymbol{r}) = z_+\rho_+(\boldsymbol{r}) + z_-\rho_-(\boldsymbol{r})$ is the charge density of the microions (of valence z_α). The polyion-microion potentials $u_{1\alpha}$ in (32) contain a hard core repulsion and a long-range Coulomb attraction (counterions) or repulsion (coions). Rapid variations of the densities profiles $\rho_\alpha(\boldsymbol{r})$ near the surfaces of the polyions, which would pose numerical problems in r-space (grid) or k-space (large $\boldsymbol{k}$ Fourier components) may be avoided by the use of appropriate classical polyion-microion pseudopotentials [15]. The correlation term F_{corr} may be expressed within the local density approximation (LDA) [15]. If it is neglected, the functional (29) reduces to the mean-field Poisson-Boltzmann (PB) form. Optimization based on the functional (29)–(32) has been achieved with the "on the fly" MD strategy for spherical polyions with counterions only (no salt) [15], and the presence if salt (i.e. with co and counterions) [31]. The effective forces between colloids are reasonably well represented by a pair-wise additive screened-Coulomb form provided the (effective) polyion charge and the screening length are treated as adjustable parameters. Other applications include rigid rod-like polyions [32], and flexible polyelectrolytes [13], the latter being investigated by MC simulations coupled with steepest descent optimization, to allow a more efficient exploration of polyelectrolyte configuration space. If F_{corr} is neglected in the functional (29), and the ideal terms are replaced by their quadratic expansion in powers of $\Delta\rho_\alpha(\boldsymbol{r}) = \rho_\alpha(\boldsymbol{r}) - \rho_\alpha$ (where ρ_α is the bulk concentration of microions), the total functional is quadratic in the $\rho_\alpha(\boldsymbol{r})$, and the Euler-Lagrange equations resulting from the extremum conditions (12) can be solved analytically [15]. The resulting total effective energy of the polyions is then strictly pair-wise additive, and the effective pair potentials are of the linearly screened DLVO form. The entire procedure is justified only for relatively weak microion inhomogeneities (i.e. $|\Delta\rho_\alpha(\boldsymbol{r})|/\rho_\alpha < 1$), i.e. for low absolute polyion valence $|Z_p|$. If the polyion charge is distributed over a number ν of interaction sites, each carrying a charge $Z_p\, e/\nu$, linear screening may be an adequate approximation for each interaction site. The resulting "Yukawa site" model, where all sites on neighbouring particles interact via a screened Coulomb (or Yukawa) pair potential, has been used to simulate charged rods [32] or charged discs representing clay particles [33].

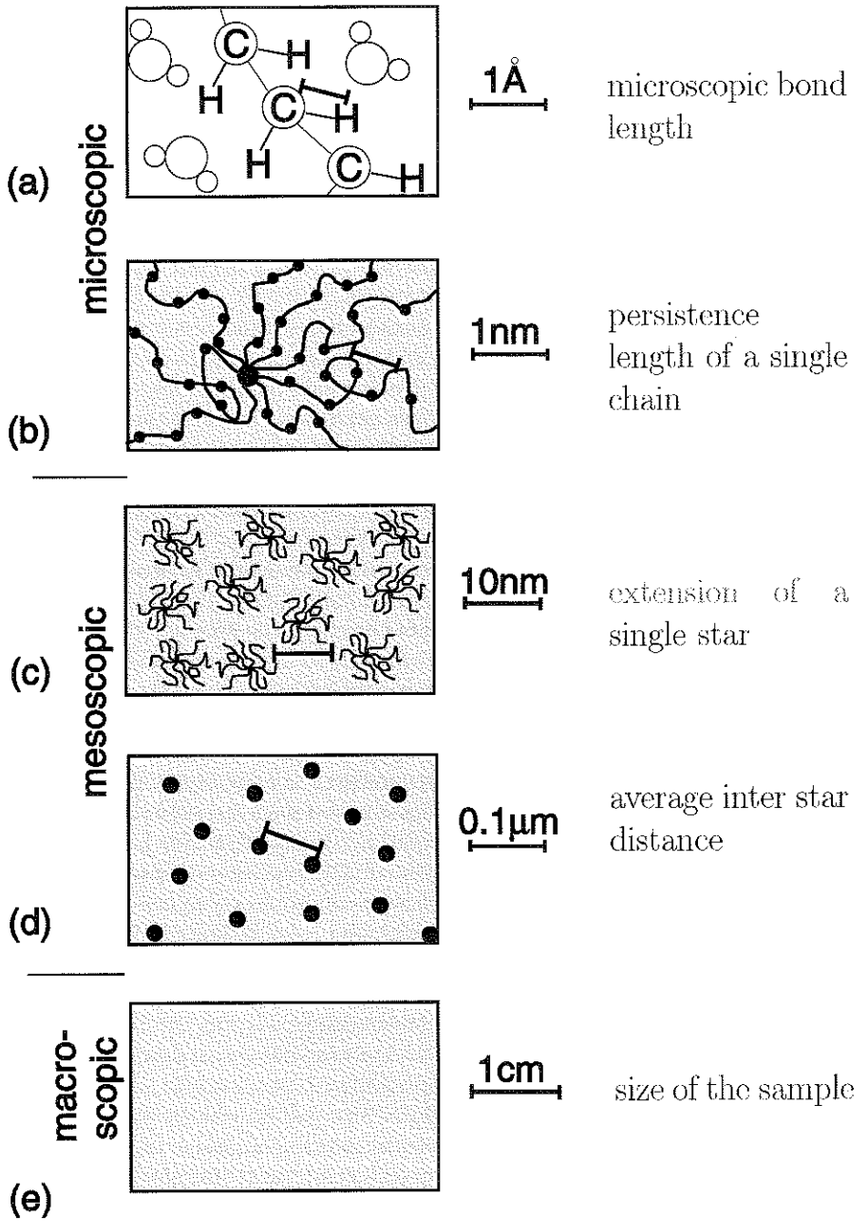

Fig. 1. Star polymer solution on different length scales. (**a**): microscopic picture, water and hydrocarbon chains are shown, the chemical bonds have a range of typically 1Å. (**b**): On a larger scale, the persistence length of the chains is relevant. (**c**): the spatial extension σ of a single polymer star. (**d**): all the coils are point particles on this scale governed by the mean intercoil distance (**e**): size of the macroscopic sample

5 Star Polymers

Star polymers [4] consist of f linear polymer chains which are chemically anchored to a common centre (f is called functionality or arm number). Obviously, linear polymers are a special case of star polymers when $f = 1, 2$ depending whether the end or middle segment is taken as "centre". Dendrimers, on the other hand, can be viewed as iterated star polymers: periodically, any linear chain branches off into n additional chains (n is called degree of branching) which is repeated g times (g is called generation number). For $f > 3$, in contrast to linear chains, star polymers and dendrimers possess a natural centre which serves as an appropriate statistical degree of freedom.

Let us first focus on *star polymers in a good solvent*. A full monomer-resolved computer simulation is completely out of reach of present-day computers: If N is the number of stars and M the number of monomers per chain, a total number of NfM particles has to be simulated, f times more than for a solution of linear chains and fM times more than for simple fluids. The strategy b) of Sect. 2, however, can be efficiently used to make progress. First consider only two stars at fixed separation r and average the force acting on their centres during an ordinary MC or MD simulation of the monomers. Such a simulation involves $2fM$ particles only. A typical simulation snapshot is shown in Fig. 2. This is repeated for different r. By integrating the distance-resolved data for the force, the effective interaction potential $v(r)$ is obtained. This interaction is repulsive, since the presence of another star reduces the number of configurations available to the chains. For small arm numbers $f \leq 10$, the simulation results confirm an effective pair potential of the log-Gauss form:

$$v(r) = \frac{5}{18} k_B T f^{3/2} \begin{cases} -\ln(\frac{r}{\sigma}) + \frac{1}{2\tau^2\sigma^2} & \text{for} \quad r \leq \sigma \ ; \\ \frac{1}{2\tau^2\sigma^2} \exp\left(-\tau^2 \frac{r^2-\sigma^2}{\sigma^2}\right) & \text{for} \quad r > \sigma \ , \end{cases} \tag{33}$$

where σ is the corona diameter of a single star measuring the spatial extent of the monomeric density. For large distances r, the interaction is Gaussian as for linear chains. It then crosses over, at the corona diameter of the star, to a logarithmic behaviour for overlapping coronae as predicted by scaling theory [34] which implies a very mild divergence as $r \to 0^+$. The matching at $r = \sigma$ is done such that the force $-dv/dr$ is continuous. In (33), $\tau(f)$ is known from a fit to computer simulation results; for $f = 2$ we obtain $\tau = 1.03$ in line with a Gaussian potential used for linear chains.

For larger arm numbers, $f > 10$, on the other hand, a geometric blob picture of f cones around the star centre, each containing one linear chain is justified [35]. The effective force for nearly touching coronae decays exponentially with r, the associated decay length is the outermost blob-diameter $2\sigma/\sqrt{f}$. This motivates a log-Yukawa form of $v(r)$ [36]:

$$v(r) = \frac{5}{18} k_B T f^{3/2} \begin{cases} -\ln(\frac{r}{\sigma}) + \frac{1}{1+\sqrt{f}/2} & \text{for} \quad r \leq \sigma \\ \frac{\sigma}{1+\sqrt{f}/2} \frac{\exp(-\sqrt{f}(r-\sigma)/2\sigma)}{r} & \text{for} \quad r > \sigma \end{cases} \tag{34}$$

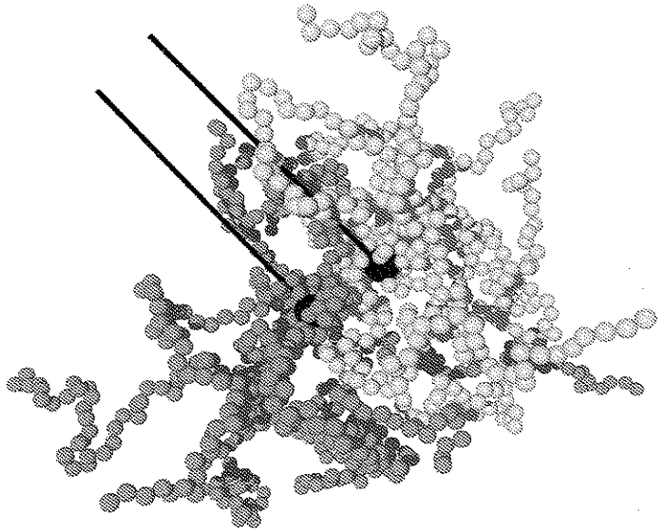

Fig. 2. Typical configuration for two stars with $f = 10$ and $M = 50$ monomers per chain as obtained from a snapshot during a Molecular Dynamics simulation. The distance between the two black lines is the centre-to-centre separation r. By courtesy of A. Jusufi

again matched at the corona diameter $r = \sigma$ such that the force is continuous. This potential was verified in monomer-resolved simulations [37] for a large range of arm numbers.

Using scaling theory and monomer-resolved simulations of a triangular configuration of three stars [38], triplet interactions were shown to be negligibly small outside the corona and at most 11 percent of the pairwise forces for penetrating triplets inside the corona; consequently the effective pair-wise description for the many-body system is adequate provided the number density ρ_s of the stars is not much higher than the overlap density $1/\sigma^3$. Large scale simulations involving many stars were performed using the pair potential of (34) [39,40]. Due the crossover of $v(r)$ at $r = \sigma$ from a harsh Yukawa to a soft logarithmic behaviour, uncommon structural and thermodynamical properties were obtained. First, the main peak of the liquid structure factor changes non-monotonically with increasing density [40]. Secondly, the bulk phase diagram exhibits [39] a reentrant melting behaviour for $34 < f < 44$ and stable anisotropic crystal lattices. The latter finding has been supported by recent experiments on various block-copolymer micelles [41–43].

Next let us briefly discuss *star polymers in a poor solvent*. The only work in this direction is close to the Θ-point where the chains are weakly interacting. Consequently the resulting effective repulsion is weaker than in good solvent. More quantitatively, an effective potential between two plates is available

within a self-consistent field approach for polymers grafted on flat plates where the grafting density is high and the self-avoidance is weak [44]. This was extended to spherical particles by employing the Derjaguin approximation [45,46] providing an analytical expression for the effective pair potential $v(r)$. In the limit of small core sizes, this expression has been successfully tested against scattering data for $f = 64$ arm stars in a solvent close to Θ conditions [47]. What is still unexplored is a systematic approach for arbitrary solvent quality which continously switches between good solvent quality to the Θ point and beyond.

Much more stretched configurations are achieved for *polyelectrolyte stars* ("porcupines") due to the strong Coulomb repulsion of the charged monomers along the chains. If one brings two polyelectrolyte stars together they hardly interdigitate but retract. A variational analysis [49] for the effective force, which includes Coulomb interactions and entropies of the counterions, reveals that the entropy of the counterions which are inside the coronae of the two polyelectrolyte stars dominates the interaction, confirming an old idea of Pincus [48]. The analytical theory was quantitatively verified by computer simulations with explicit monomers and counterions [49]. Inside the corona, the resulting effective force could be fitted by an inverse-power law $\propto r^{-\gamma}$ where the exponent γ slightly depends on the actual charging conditions but is always around $0.7 - 0.8$. By integration, an effective potential is obtained which stays finite at the origin and behaves inside the corona as $v(r) = v(0) - Cr^{1-\gamma}$ with a positive constant C. However, the actual value $v(0)$ for completely overlapping stars is much larger than k_BT so that significant overlap is rare. Due to the softness of the interaction, similar structural anomalies as obtained for star polymers are expected including a non-monotonic variation of the first peak in the structure factor for increasing density and reentrant melting.

6 Colloids and Polymers: Depletion Interactions

If a sterically-stabilized colloidal particle is brought into a non-adsorbing polymer solution, the latter are depleted in a zone around the colloidal surfaces due to the colloid-polymer repulsion. The width of this zone is of the order of the radius of gyration $d_p/2$ of the polymers. If one now brings two colloidal particles close to each other, the two depletion zones overlap, which brings about a free energy gain of the polymers relative to a situation of non-overlapping zones, resulting in an effective attraction between the colloids, the so-called depletion attraction. Alternatively one can view the attraction arising from an unbalanced osmotic pressure exerted on the colloidal particles by the surrounding polymers.

The simplest model for colloid-polymer mixtures including the depletion effect is the so-called Asakura-Oosawa (AO) [50] or Asakura-Oosawa-Vrij (AOV) [51] model which assumes hard core interactions between the colloids of diameter d_c, further hard-core interactions between the polymers and the

colloids with a range $(d_c + d_p)/2$, but no interaction at all between polymers. The ideality of the polymers is a crucial approximation which is fulfilled only for dilute polymer solutions, but it allows to investigate many of the statistical properties of the AO model analytically. For instance, the effective interaction $v(r)$ between a colloidal pair can be calculated to be the product of the polymer osmotic pressure $P_p = k_B T \rho_p$ and the overlap volume of the two depletion zones consisting of two spherical half-caps. Explicitly it reads

$$\frac{v(r)}{k_B T} = \begin{cases} \infty & \text{for} \quad r \le d_c \\ \rho_p \frac{\pi}{6}(d_c + d_p)^3 \left[1 - \frac{3r}{2(d_c+d_p)} + \frac{1}{2}\frac{r^3}{(d_c+d_p)^3}\right] & \text{for} \quad d_c < r \le d_c + d_p \\ 0 & \text{for} \quad r \ge d_c + d_p \end{cases} \tag{35}$$

Furthermore, by a simple geometric consideration, it can be shown that effective triplet and higher-order many-body forces vanish provided the size ratio between colloids and polymers $q = d_p/d_c$ is smaller than 0.154. In this case, the AO model is formally equivalent to an effective one-component system with a short ranged attraction, which immediately opens the way for large-scale simulations.

The phase diagram of the AO model was explored by computer simulations on two different levels: first, one-component calculations using the effective pair potential (35) have been performed [52], which are exact for $q < 0.154$. Secondly, more recently, Dijkstra has simulated the full effective Hamiltonian including effective many-body forces to arbitrary order for $q = 1$ [53]. The emerging phase diagram involves three phases: gas (i.e. colloidal poor), liquid (i.e. colloidal rich) and an fcc colloidal crystal. A liquid phase is stable if the ratio q is larger than $q_c \approx 0.5$.

On the other hand, theoretical progress was made by constructing a free volume theory for the fluid bulk free energies [54] which provides a reliable estimate for the gas-liquid transition. A free-energy density functional for the AO colloid-polymer mixtures, valid for arbitrary inhomogeneous situations, was constructed [55] in the spirit of Rosenfeld's fundamental measure approach [19], which reproduces the effective interaction (35) for a colloid pair and the free volume theory of [54]. This density functional was applied to wetting phenomena of planar walls. A novel type of wetting involving growth of only few colloidal liquid layers on top of the wall as liquid-gas coexistence is approached was predicted by density functional theory [56] and confirmed by computer simulations [53]. This wetting scenario only shows up for ratios larger than q_c, so that one can speculate that it is produced by the intrinsic many-body nature of the effective forces.

Obviously, the AO model has the short-coming of idealized interactions. More realistic models involve a non-zero polymer-polymer interaction and a softer polymer-wall interaction [57]. On the other hand, full two-component

simulations of colloids and polymers were performed [58, 59] where the polymers are defined on a lattice. Clearly these include any effective many-body interactions. A second computationally less demanding technique is to calculate effective pair interactions between a colloid and a polymer first by a monomer-resolved reference simulation. This strategy was followed in the more general context of mixtures of colloids and star polymers for small size ratios q. Supported by theoretical scaling arguments the following pair interaction between a hard-sphere colloid and a star polymer was obtained [60, 61]:

$$v_{cp}(r) = k_B T \Lambda f^{3/2} \left(\frac{d_c}{2r + d_c}\right) \times \begin{cases} -\ln\left(\frac{2r-d_c}{\sigma}\right) + \left(\frac{(2r-d_c)^2}{\sigma^2} - 1\right)((1+4\kappa)/(1+2\kappa)) + \zeta & \text{for } r \le (d_c+\sigma)/2; \\ \zeta \operatorname{erfc}(\kappa(2r-d_c)/\sigma)/\operatorname{erfc}(\kappa) & \text{else,} \end{cases} \tag{36}$$

Here, Λ and κ are known parameters depending on the functionality f of the star, $\zeta = \sqrt{\pi}\operatorname{erfc}(\kappa)\exp(\kappa^2)/(\kappa(1+2\kappa^2))$, σ denotes the corona diameter of the star and $\operatorname{erfc}(x)$ is the complementary error function. For $r \to d_c/2$ the potential diverges logarithmically as for the star-star interaction (33). Linear polymer chains are obtained as the special case $f = 2$ where $\Lambda = 0.46$ and $\kappa = 0.58$. The two-component system with effective pair interactions was investigated in detail by further simulation and liquid integral equation theory. For different arm numbers f, the fluid-fluid demixing transition was calculated [60] in good agreement with experimental data. Furthermore, the freezing transitions was discussed. Above a critical arm number of $f_c \approx 10$, fluid-fluid demixing was preempted by freezing [62]. More recently, the fluid-fluid interfacial tension was calculated on the basis of the realistic effective interactions between colloids and linear polymers (being the special case $f = 1$ in (35) [63].

In case of polymer size comparable or larger than the colloidal diameter d_c, effective many-body forces play a significant role. Complementary methods such as monomer-resolved liquid intergral equations methods combined with the PRISM approach [64] or field-theoretic calculations [65] have provided valuable insight into the structure of colloid-polymer mixtures. The limit of large q contains completely different physics, since the colloidal spheres represent then small perturbations for the long polymer chains [59].

7 Conclusions

In conclusion, we have demonstrated that the concept of effective interactions allows large-scale simulations and provides additional insight into the physical mechanisms governing colloidal dispersions and polymer solutions.

The open problems are in the application of effective interaction to dynamical questions both in equilibrum and nonequilibrium [66]. This is much

harder to establish since there is no clean statistical mechanics guideline in this case.

Acknowledgements

I thank J. P. Hansen, E. Allahyarov, J. Dzubiella, A. Jusufi, C. N. Likos, A. A. Louis and A. Lahcen for help and for valuable comments.

References

1. For a recent review, see: T. A. Witten (1999) Insights from soft condensed matter. *Rev. Mod. Phys.* **71**, pp. S367–S373
2. R. J. Hunter (1989) *Foundations of Colloid Science* Volume I, Oxford Science Publications, Clarendon Press, Oxford
3. See e.g.: S. Neser, C. Bechinger, P. Leiderer, T. Palberg (1997) Finite-Size Effects on the Closest Packing of Hard Spheres. *Phys. Rev. Letters* **79**, pp. 2348–2351
4. For a review see: G. S. Grest, L. J. Fetters, J. S. Huang, D. Richter (1996) Star Polymers: Experiment, theory and simulation. *Advances in Chemical Physics* Volume **XCIV**, p. 67
5. J.-P. Hansen, H. Löwen (2002) *Effective interactions for large-scale simulations of complex fluids,* in: Bridging Time Scales: Molecular Simulations for the Next Decade P. Nielaba, M. Mareschal, G. Ciccotti (Eds.), Springer, Berlin, pp. 167–198, ISBN 3-540-44317-7
6. C. N. Likos (2001) Effective interactions in soft condensed matter physics. *Physics Reports* **348**, pp. 267–439
7. L. Belloni (2000) Colloidal interactions. *J. Phys.: Condens. Matter* **12**, pp. R549–R587
8. J. P. Hansen, H. Löwen (2000) Effective interactions between electric double-layers. *Ann. Rev. Phys. Chem.* **51**, pp. 209–242
9. M. Dijkstra (2001) Computer simulations of charge and steric stabilised colloidal suspensions. *Current Opinion in Colloid and Interface Science* **6**, pp. 372–382
10. See e.g. R. van Roij, M. Dijkstra, J. P. Hansen (1999) Phase diagram of charge-stabilized colloidal suspensions: van der Waals instability without attractive forces. *Phys. Rev. E* **59**, pp. 2010–2025
11. H. Löwen (1994) Melting, freezing and colloidal suspensions. *Phys. Reports* **237**, pp. 249–324
12. For an extensive review of classical DFT see R. Evans in Fundamentals of Inhomogeneous Fluids. edited by D. Henderson (Marcel Decker, New York, 1992)
13. J. P. Hansen and E. Smargiassi (1996) in Monte Carlo and Molecular Dynamics of Condensed Matter Systems, edited by K. Binder and G. Ciccotti Societa Italiana di Fisica, Bologna
14. See e.g. G. Galli and M. Parrinello (1991) in Computer Simulations in Materials Science. P. 282, edited by M. Meyer and V. Pontikis Kluwer, Dordrecht
15. H. Löwen, J. P. Hansen, P. A. Madden (1993) Nonlinear counterion screening in colloidal suspensions. *J. Chem. Phys.* **98**, pp. 3275–3289

16. F. Gygi, G. Galli (1995) Real-space adaptive-coordinate electronic-structure calculations. *Phys. Rev. B* **52**, pp. R2229–R2232
17. R. Roth, R. Evans, S. Dietrich (2000) Depletion potential in hard-sphere mixtures: Theory and applications. *Phys. Rev. E* **62**, pp. 5360–5377
18. D. Goulding, S. Melchionna (2001) Accurate calculation of three-body depletion interactions. *Phys. Rev. E* **64**, p. 011403 (1-9)
19. Y. Rosenfeld, M. Schmidt, H. Löwen, P. Tarazona (1997) Fundamental-measure free energy density functional for hard spheres: Dimensional crossover and freezing. *Phys. Rev. E* **55**, pp. 4245-4263
20. H. Löwen (2000) in: "Spatial Statistics and Statistical Physics", edited by K. Mecke and D. Stoyan, Springer Lecture Notes in Physics **554**, pp. 295–331, Berlin
21. A. Lang, C. N. Likos, M. Watzlawek, H. Löwen (2000) Fluid and solid phases of the Gaussian core model. *J. Phys.: Condensed Matter* **12**, pp. 5087–5108
22. C. N. Likos, A. Lang, M. Watzlawek, H. Löwen (2001) Criterion for determining clustering versus reentrant melting behavior for bounded interaction potentials. *Phys. Rev. E* **63**, p. 031206 (1-9)
23. A. A. Louis (2000) Effective potentials for polymers and colloids: beyond the van der Waals picture of fluids? *Philos. Trans. R. Soc. Lond. A* **359**, pp. 939–960
24. M. Schmidt (1999) Density-functional theory for soft interactions by dimensional crossover. *Phys. Rev. E* **60**, pp. R6291–R6294
25. B. V. Derjaguin, L. D. Landau (1948) Acta Physicochim. USSR **14**, 633 (1941); E. J. W. Verwey and J. T. G. Overbeek, *Theory of the Stability of Lyophobic Colloids.* Elsevier, Amsterdam
26. A. Delville, R. J. M. Pellenq (2000) Electrostatic attraction and/or repulsion between charged colloids : a (NVT) Monte-Carlo study, Molecular Simulation **24**, pp. 1–24; R. Messina, C. Holm, K. Kremer (2000) Strong Attraction between Charged Spheres due to Metastable Ionized States. *Phys. Rev. Lett.* **85**, pp. 872–875; T. Terao, T. Nakayama (2001) Charge inversion of colloidal particles in an aqueous solution: Screening by multivalent ions *Phys. Rev. E* **63**, 041401 (1–6); B. Hribar, V. Vlachy (2001) A Monte Carlo Study of Micellar Solutions with a Mixture of Mono- and Trivalent Counterions. *Langmuir* **17**, pp. 2043–2046
27. A. Delville (1999) (N,V,T) Monte Carlo Simulations of the Electrostatic Interaction between Charged Colloids: Finite Size Effects. *J. Phys. Chem. B* **103**, pp. 8296–8300; A. Delville, P. Levitz (2001) Direct Derivation of the Free Energy of Two Charged Lamellar Colloids from (N,V,T) Monte Carlo Simulations. *J. Phys. Chem. B* **105**, pp. 663–667
28. H. Löwen, E. Allahyarov (1998) The role of effective triplet interactions in charged colloidal suspensions. *J. Phys.: Condensed Matter* **10**, pp. 4147–4160
29. R. D. Groot (1991) Ion condensation on solid particles: Theory and simulations. *J. Chem. Phys.* **95**, pp. 9191–9203
30. M. J. Stevens, M. L. Falk, M. O. Robbins (1996) Interactions between charged spherical macroions. *J. Chem. Phys.* **104**, pp. 5209–5219
31. H. Löwen, G. Kramposthuber (1993) Optimal effective pair potential for charged colloids. *Europhys. Lett.* **23**, pp. 673–678
32. H. Löwen (1994) Interaction between charged rod-like colloidal particles. *Phys. Rev. Lett.* **72**, pp. 424–427; (1994) Charged rod-like colloidal suspensions: an ab initio approach. *J. Chem. Phys.* **100**, pp. 6738–6749

33. S. Kutter, J. P. Hansen, M. Sprik, E. Boek (2001) Structure and phase behavior of a model clay dispersion: A molecular-dynamics investigation. *J. Chem. Phys.* **112**, pp. 311–322
34. T. A. Witten, P. A. Pincus (1986) Colloid Stabilization by Long Grafted Polymers. *Macromolecules* **19**, pp. 2509–2513
35. M. Dauod, J. P. Cotton (1982) Star Shaped Polymers: A Model for the Conformation and Its Concentration Dependence. *J. Phys. (Paris)* **43**, pp. 531–538
36. C. N. Likos, H. Löwen, M. Watzlawek, B. Abbas, O. Jucknischke, J. Allgaier, D. Richter (1998) Star Polymers Viewed as Ultrasoft Colloidal Particles. *Phys. Rev. Letters* **80**, pp. 4450–4453
37. A. Jusufi, M. Watzlawek, H. Löwen (1999) Effective Interaction between Star Polymers. *Macromolecules* **32**, pp. 4470–4473
38. C. von Ferber, A. Jusufi, C. N. Likos, H. Löwen, M. Watzlawek (2000) Triplet interactions in star polymer solutions. *Europhys. Journal E* **2**, pp. 311–318
39. M. Watzlawek, C. N. Likos, H. Löwen (1999) Phase Diagram of Star Polymer Solutions. *Phys. Rev. Letters.* **82**, pp. 5289–5292
40. M. Watzlawek, H. Löwen, C. N. Likos (1998) The anomalous structure factor of dense star polymer solutions. *J. Phys.: Condensed Matter* **10**, pp. 8189–8205
41. G. A. McConnell, A. P. Gast (1997) Melting of Ordered Arrays and Shape Transitions in Highly Concentrated Diblock Copolymer Solutions. *Macromolecules* **30**, pp. 435–444
42. T. P. Lodge, J. Bang, M. J. Park, K. Char (2004) Origin of the Thermoreversible fcc-bcc Transition in Block Copolymer Solutions. *Phys. Rev. Lett.* **92**, p. 145501 (1-4)
43. M. Laurati, J. Stellbrink, R. Lund, L. Willner, D. Richter, E. Zaccarelli (2005) Starlike Micelles with Starlike Interactions: A Quantitative Evaluation of Structure Factors and Phase Diagram. *Phys. Rev. Lett.* **94**, p. 195504 (1-4)
44. S. T. Milner, T. A. Witten, M. E. Cates (1988) Theory of the Grafted Polymer Brush. *Macromolecules* **21**, pp. 2610–2619
45. J. Mewis, W. J. Frith, T. A. Strivens, W. B. Russel (1989) The rheology of suspensions containing polymerically stabilized particles. *A. I. Ch. E. J.* **35**, pp. 415–422
46. U. Genz, B. D'Aguanno, J. Mewis, R. Klein (1994) Structure of Sterically Stabilized Colloids. *Langmuir* **10**, pp. 2206–2212
47. C. N. Likos, H. Löwen, A. Poppe, L. Willner, J. Roovers, B. Cubitt, D. Richter (1998) Ordering phenomena of star polymer solutions approaching the Θ state. *Phys. Rev. E* **58**, pp. 6299–6307
48. P. Pincus (1991) Colloid Stabilization with Grafted Polyelectrolytes. *Macromolecules* **24**, pp. 2912–2919
49. A. Jusufi, C. N. Likos, H. Löwen (2002) Conformations and Interactions of Star-Branched Polyelectrolytes. *Phys. Rev. Letters* **88**, p. 018301 (1-4)
50. S. Asakura, F. Oosawa (1954) On Interaction between Two Bodies Immersed in a Solution of Macromolecules. *J. Chem. Phys.* **22**, pp. 1255–1256
51. A. Vrij (1976) Polymers at interfaces and the interactions in colloidal dispersions. *Pure Appl. Chem.* **48**, pp. 471–483
52. M. Dijkstra, J. M. Brader, R. Evans (1999) Phase behaviour and structure of model colloid-polymer mixtures. *J. Phys.: Condensed Matter* **11**, pp. 10079–10106

53. M. Dijkstra, R. van Roij (2002) Entropic Wetting and Many-Body Induced Layering in a Model Colloid-Polymer Mixture. *Phys. Rev. Letters* **89**, p. 208303 (1–4)
54. H. N. W. Lekkerkerker, W. C. K. Poon, P. N. Pusey, A. Stroobants, P. B. Warren (1992) Phase behaviour of colloid+polymer mixtures. *Europhys. Lett.* **20**, pp. 559–564
55. M. Schmidt, H. Löwen, J. M. Brader, R. Evans (2000) Density Functional for a Model Colloid-Polymer Mixture. *Phys. Rev. Letters* **85**, pp. 1934–1937
56. M. Schmidt, H. Löwen, J. M. Brader, R. Evans (2002) Density functional theory for a model colloid-polymer mixture: bulk fluid phases. *J. Phys.: Condensed Matter* **14**, pp. 9353–9382
57. A. A. Louis, R. Finken, J. P. Hansen (2000) Crystallization and phase separation in nonadditive binary hard-sphere mixtures. *Rev. Phys. E* **61**, pp. R1028–R1031
58. E. J. Meijer, D. Frenkel (1995) Computer simulation of colloid-polymer mixtures. *Physica A* **213**, pp. 130–137
59. A. Johner, J. F. Joanny, S. Diez Orrite, J. Bonet Avalos (2001) Gelation and phase separation in colloid-polymer mixtures. *Europhys. Letters* **56**, pp. 549–555
60. J. Dzubiella, A. Jusufi, C. N. Likos, C. von Ferber, H. Löwen, J. Stellbrink, J. Allgaier, D. Richter, A. B. Schofield, P. A. Smith, W. C. K. Poon, P. N. Pusey (2001) Phase separation in star polymer-colloid mixtures. *Phys. Rev. E* **64**, p. 01040 (1–4)
61. A. Jusufi, J. Dzubiella, C. N. Likos, C. von Ferber, H. Löwen (2001) Effective interactions between star polymers and colloidal particles. *J. Phys.: Condensed Matter* **13**, pp. 6177–6194
62. J. Dzubiella, C. N. Likos, H. Löwen (2002) Star-polymers as depleting agents of colloidal hard spheres. *Europhys. Letters.* **58**, pp. 133–139
63. R. L. C. Vink, A. Jusufi, J. Dzubiella, C. N. Likos (2005) Bulk and interfacial properties in colloid-polymer mixtures. *Phys. Rev. E* **72**, p. 030401 (1–4)
64. M. Fuchs, K. S. Schweizer (2001) Macromolecular theory of solvation and structure in mixtures of colloids and polymers. *Phys. Rev. E* **64**, p. 021514 (1–19)
65. A. Hanke, E. Eisenriegler, S. Dietrich (1999) Polymer depletion effects near mesoscopic particles. *Phys. Rev. E* **59**, pp. 6853–6878
66. H. Löwen (2001) Colloidal soft matter under external control. *J. Phys.: Condensed Matter* **13**, pp. R415–R432